WALL TURBULENCE AT HIGH FRICTION REYNOLDS NUMBERS

Sergio Hoyas
IUMPA, Universitat Politècnica de València,
València, Spain, serhocal@mot.upv.es

Martin Oberlack
TU Darmstadt, Chair of Fluid Dynamics,
Darmstadt, Germany, oberlack@fdy.tu-darmstadt.de

ABSTRACT

A new direct numerical simulation of Poiseuille channel flow with a frictional Reynolds number of $10,000$ was performed using the LISO pseudospectral code. The mean flow presents a long logarithmic layer ranging from 400 to 2500 wall units, longer than expected. The maximum intensity of the flow velocity increases with the Reynolds number. The elusive second maximum of this intensity is also yet to appear. If it existed, its position would be around $y^+ \approx 120$, extrapolating the friction Reynolds number to around 13500. For several Reynolds numbers, this slight difference in the near-wall gradient of the intensity is associated with a scaling failure of dissipation, confirming this hypothesis. The scaling of the turbulent users in the middle of the channel is almost perfect above 1000 wall units. Finally, the peak pressure intensity grows with increasing Reynolds number and does not scale in wall units.

INTRODUCTION

After almost 140 years of the publication of O. Reynolds's first work, turbulence is still an open problem. Research of turbulent flows has been dominated by experimental techniques until the eighties of the last century, where supercomputers started to be powerful enough to solve the equations of turbulent flows. In fact, Direct Numerical Simulation (DNS) has become one of the main tools in studying wall turbulence. However, DNSs are extremely expensive in terms of computational resources. Thus, the most studied configurations have been turbulent boundary layers and channels. Here we study the later, where the fluid is confined between two parallel plates and the flow is driven by pressure.

The friction Reynolds number, defined as $Re_\tau = u_\tau h/\nu$, is the main control parameter in wall bounded turbulence. Here $u_\tau = \sqrt{\tau_w/\rho}$ is the friction velocity, ν is the kinematic viscosity, ρ is the density, and τ_w is the friction at the wall. h is the semi-height of the channel and is equivalent to the radius in pipes and δ_{99} in boundary layers. Since the seminal work of Kim, Moin and Moser Kim *et al.* (1987), the Re_τ has steadily increased from 180 in 1987 to 8000 in 2018 (Kim *et al.*, 1987; Hoyas & Jiménez, 2006; Lozano-Durán & Jiménez, 2014; Bernardini *et al.*, 2014; Yamamoto & Tsuji, 2018). A simulation reaching the $Re_\tau = 10000$ frontier is presented here. This simulation has been very recently published, and some more details are given here: Oberlack *et al.* (2022); Hoyas *et al.* (2022).

This friction Reynolds number is less than the largest realisation of the flow obtained by experimental means, see Samie *et al.* (2018) and discussion inside. In particular, Samie *et al.* (2018) reached a value of $20,000$ with very good spatial resolution. The main advantage, however, is that DNS allows the computation of any conceivable quantity over the entire domain, including derivatives close to walls. In addition to contributing to discussions on some of the issues that have arisen over the past few years, with this simulation we are providing community data that hopefully will help better model turbulence.

In the present article we will restrict ourselves to present the data and the kinematics of the flow, referring the interested reader to Oberlack *et al.* (2022) for scaling laws about the streamwise mean velocity. This work is organized as follows. Section two describes the numerical method and the validation of the data. Section three discusses the one-point statistics of the flow, including mean flow and intensities. The energy turbulent budgets are discussed in section four. Finally, section five contains the conclusions of this work.
The database containing the mean flow, intensities, and turbulent budgets can be downloaded from the TUdatalib Repository of TU Darmstadt at https://doi.org/10.48328/tudatalib-658

Numerical method

In this work we present the results of a DNS of a pressure-driven (Poiseuille) channel flow at a nominal $Re_\tau = 10000$. Superscript (+) indicates that the quantities have been normalized by u_τ and ν. This simulation has been performed in a computational box of sizes $L_x = 2\pi h$, $L_y = 2h$ and $L_z = \pi h$. For Poiseuille flow, Lozano-Durán & Jiménez (2014) noticed that even relatively small computational boxes of stream- and spanwise sizes of only $2\pi h \times \pi h$ can satisfactorily recover the one-point statistics of the flow. The streamwise, wall-normal, and spanwise coordinates are $x, y,$ and z, respectively. The corresponding velocity components are U, V and W or, using index notation, U_i. Statistically averaged quantities in time, x and z are denoted by an overbar, $\overline{U}$, whereas fluctuating quantities are denoted by lowercase letters, i. e., $U = \overline{U} + u$. Primes are reserved for intensities, $u' = \overline{uu}^{1/2}$.

The Navier-Stokes equations have been solved using the LISO code, which has successfully been employed to run some

Case	Line	Re_τ	Re_b	L_x	L_z	Δx^+	Δz^+	Tu_τ/h
HJ02	······	2000	43650	$8\pi h$	$3\pi h$	12.3	6.1	11
LJ04	- - - -	4000	98302	$2\pi h$	πh	12.8	6.4	15
LM05	-·-·-	5200	125000	$8\pi h$	$3\pi h$	8.2	4.1	7.80
HO10	——	10000	261000	$2\pi h$	πh	15.3	7.6	19.8

Table 1: Parameters of the simulations. Re_b is the bulk Reynolds number, $Re_b = U_b h/\nu$, where U_b is the bulk velocity. Δ_x^+ and Δ_z^+ are in terms of dealiased Fourier modes. The last column is the total simulation time in terms of eddy turnovers.

of the largest simulations of turbulence (Hoyas & Jiménez, 2006; Avsarkisov *et al.*, 2014*a*,*b*; Kraheberger *et al.*, 2018; Alcántara-Ávila *et al.*, 2021). Briefly, the code uses the same strategy than Kim *et al.* (1987), but using a seven-point compact finite differences in y direction with fourth-order consistency and extended spectral-like resolution (Lele, 1992). The temporal discretization is a third-order semi-implicit Runge-Kutta scheme (Spalart *et al.*, 1991). The wall-normal grid spacing is adjusted to keep the resolution at $\Delta y = 1.5\eta$, i.e., approximately constant in terms of the local isotropic Kolmogorov scale $\eta = (\nu^3/\varepsilon)^{1/4}$. In wall units, Δy^+ varies from 0.3 at the wall, up to $\Delta y^+ \simeq 12$ at the centerline. The resolution in x and z is similar to the largest simulations of turbulence, see table 1. A code similar to the one used presently, including the energy equation, is explained in Lluesma-Rodríguez *et al.* (2021).

The initial file of this simulation was taken from a smaller Reynolds number simulation. To accelerate the compilation of statistics, three initial files were prepared and thus three simulations were run at the same time. In every case, the code was run until some transition phase had passed and the flow had adjusted to the new set of parameters. Once the flow was in a statistically steady state, statistics were compiled. The running times to compile statistics are shown in terms of eddy-turnovers in the rightmost column of table 1. The transitions until the simulations reached a statistically steady state, which were very time consuming, are not contemplated in this table.

Table 1 also shows the parameters of the simulations HJ02 (Hoyas & Jiménez, 2006), LJ04 (Lozano-Durán & Jiménez, 2014), and LM05 (Lee & Moser, 2015). These simulations will be used in the paper in the colour code described in the second column of table 1. As it is said above, this code has already proved its worth, but to further validate the statistics, figure 1 shows the error in the momentum equation,

$$\frac{d\overline{U}^+}{dy^+} - \overline{uv}^+ = 1 - y^+. \tag{1}$$

The difference between both sides of this equation is below 2×10^{-3}, similar to the other tree simulations utilized here. Thus, it has been considered that enough statistical information was obtained.

One point statistics

The mean velocity profile is shown in figure 2a in terms of the indicator function, $\Gamma = y^+\partial_{y^+}\overline{U}^+$. This function should show a plateau if the classical scaling for the logarithmic layer $\overline{U}^+ = \kappa^{-1}\log(y^+) + B$ holds, where κ is the von Kármán constant. Moreover, in Oberlack *et al.* (2022) it is shown that the

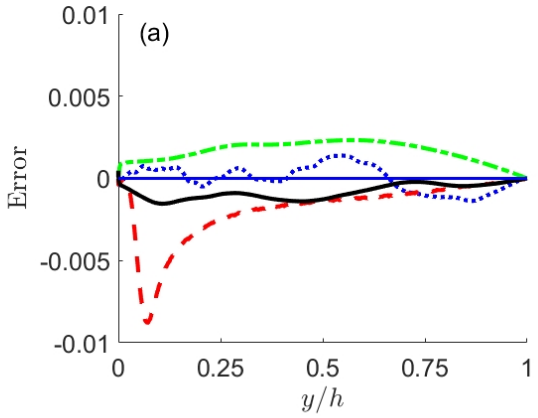

Figure 1: Error in the computation of momentum equation (1)

profile of $\overline{U}^+$ is indeed logarithmic, using the Lie-symmetry theory applied to turbulence. Furthermore, it this article it is shown that in the log-region we have

$$U_1^+ = \frac{1}{\kappa}\ln\left(y^+\right) + B, \tag{2}$$

$$(U_1^n)^+ = C_n\left(y^+\right)^{\omega(n-1)} - B_n, \text{for}\, n \geq 2, \tag{3}$$

$$C_n = \alpha e^{\beta n}, B_n = \tilde{\alpha} e^{\tilde{\beta} n}, \text{ for } n \geq 2. \tag{4}$$

where κ, B, B_n, C_n, α, β, $\tilde{\alpha}$ and $\tilde{\beta}$ are constants that need to be fitted with experiments. For several of the flows analysed, $\omega = 0.10$.

For every case, the first local minimum of Γ is reached around $y^+ \approx 70$, which more or less coincide with the classic starting point of the logarithmic layer (Pope, 2000). However, the indicator function is not flat until $y^+ \approx 400$, so this could be a new starting point. The logarithmic layer extends to around $y^+ \approx 2500$ or $y/h = 0.25$, above the usual value of $y/h = 0.2$. To obtain the values of κ and B, we have restricted ourselves to the region where the indicator function is flattest, i.e., from $y^+ = 400$ to $y/h = 0.25$ (figure 2a), obtaining $\kappa = 0.394$ and $B = 4.61$. This value of κ is similar to the experimental one of Marusic *et al.* (2013), and only 0.010 and 0.007 units larger than the one given by Lee & Moser (2015) and Yamamoto & Tsuji (2018). Abe & Antonia (2016) also obtained this value in their study of global energy. Studying the finite Reynolds number effects on the flow, Luchini (2017), and Spalart & Abe (2021), give a similar value.

It is worth mentioning that some other authors, with dif-

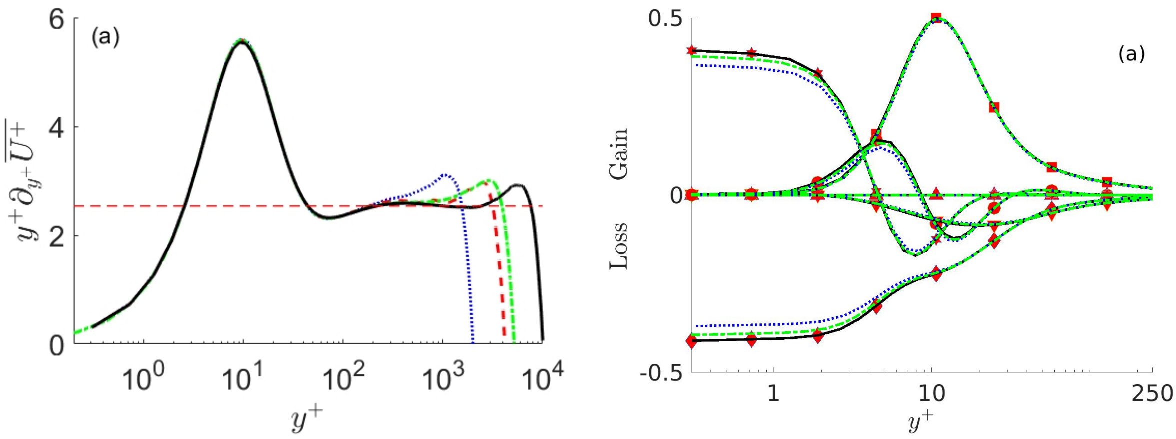

Figure 2: Lines as in table 1. (a) Indicator function, showing a log layer in the range $y^+ = 400 - 2500$. (b) Budgets for Reynolds stresses in wall units. Production ■, dissipation ⧫, viscous diffusion $*$, pressure-strain ▼, pressure diffusion ▲, turbulent diffusion •.

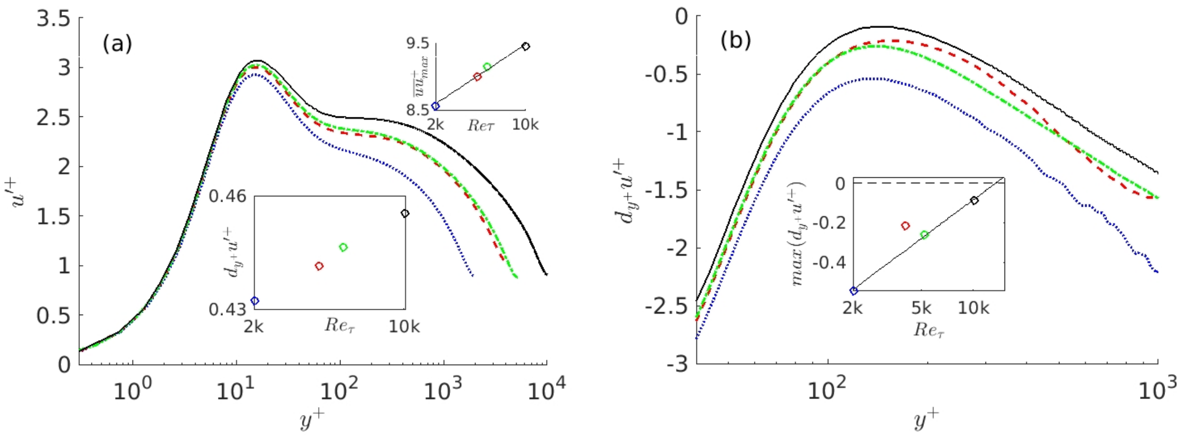

Figure 3: Lines as in table 1. (a) u'^+. Box: $d_{y^+}u'^+$ evaluated at the wall. (b) $d_{y^+}u'^+$, close to the possible second maximum. Box: maximum value of $d_{y^+}u'^+$

ferent tools, have obtained values above 0.40. McKeon McKeon *et al.* (2004) in high Reynolds numbers involving pipes got 0.42. More recently, Monkewitz (2021) has developed an algorithm to model $\overline{U}^+$ for very large Reynolds numbers. The value of κ is similar to the one obtained by us. However, in Monkewitz (2021) the actual logarithmic profile for $Re_\tau = 10^5$ would start around 10^3 wall units for a final value $\kappa = 0.42$. As a DNS reaching this Re_τ is approximately 3500 times more costly than the one presented here, this is probably an open problem for the next decade or more.

The intensity of the streamwise velocity, u'^+, is shown in figure 3a. The well known scaling failure in the buffer layer is still present (Hoyas & Jiménez, 2006), and the maximum of the intensity is $u'^+ = 3.07$. About the open question of a possible second maximum of u'^+ the situation is shown in figure 3b. If it exists, this maximum would be located around $y^+ \approx 120$. However, the derivative of u'^+ is still not zero. Fitting the data to a logarithmic grow law, we obtain $d_y u_0'^+ = 0.29 \log Re_\tau - 2.7$, and a approximate critical value of $Re_\tau = 13500$.

The scaling failure of the dissipation

The budget equation for the component $\overline{u_i u_j}$ of the Reynolds-stress tensor is written as Mansour *et al.* (1988); Hoyas & Jiménez (2008)

$$B_{ij} \equiv D\overline{u_i u_j}/Dt = P_{ij} + \varepsilon_{ij} + T_{ij} + \Pi^s_{ij} + \Pi^d_{ij} + V_{ij}. \qquad (5)$$

The terms in the right hand side of equation (5) are referred as production, dissipation, turbulent diffusion, viscous diffusion, pressure-strain, and pressure-diffusion.

$$\begin{aligned} P_{ij} &= -\overline{u_i u_k}\partial_k \overline{U_j} - \overline{u_j u_k}\partial_k \overline{U_i}, & \varepsilon_{ij} &= -2\nu\overline{\partial_k u_i \partial_k u_j}, \\ T_{ij} &= \partial_k \overline{u_i u_j u_k}, & V_{ij} &= \nu\partial_{kk}\overline{u_i u_j} \\ \Pi^s_{ij} &= \overline{p(\partial_j u_i + \partial_j u_i)}, & \Pi^d_{ij} &= \partial_k\left(\overline{p u_i}\delta_{jk} + \overline{p u_j}\delta_{ik}\right), \end{aligned}$$

where δ_{ij} is Kronecker's delta. The splitting of the pressure in two different terms is not unique, but this one offers more information in the B_{12} and B_{22} terms (Hoyas & Jiménez, 2008). Finally, in channels $B_{ij} \equiv 0$. In the viscous and buffer layers, budgets should scale in wall units, $B^+_{ij} = B_{ij}\nu/u^3_\tau$. The B_{11} budget is shown in figure 3b, using this scale. Except those terms that are identically zero, all are active. The well-known scaling failure (Hoyas & Jiménez, 2008) of the dissipation at the wall for B_{11} is still present. As expected all terms collapse for

$y^+ > 10$. However, below this more or less arbitrary limit, the absolute values of ε_{11}^+ and V_{11}^+ increase with the Reynolds number. This scaling failure can be linked to the growing of the first maximum of u'^+. At the wall (Hoyas & Jiménez, 2008),

$$V_{11}|_{y=0} = \nu \partial_{yy} \overline{u^2}|_{y=0} = 2\nu \overline{(\partial_y u)^2}|_{y=0} = -\varepsilon_{11} \qquad (6)$$

as all other terms vanish. u'^+ can be approximated by $u'^+ = \left(b_u y^+ + c_u {y^+}^2 + ...\right)$. Therefore, near the wall, $u'^+ \approx b_u y^+$, and $V_{11}^+ \approx b_u^2$. Thus, the reason why this term of the turbulent budget does not scale with the Reynolds number in the wall comes from the differences in the b_u terms. This term represents the slope of u'^+ near the wall. Looking at the box in figure 3a, one can see that, effectively, the value of du'^+/dy^+ at the wall does not collapse, but slightly increase. Apart from our data, there are evidences that the peak at $y^+ \approx 15$ keeps growing with respect to Re_τ (Samie *et al.*, 2018). Because the position of the peak is constant in y^+, the slope of u'^+ has to be higher for larger Re_τ. In other words, as long as the peak of u'^+ increases with Re_τ, b_u will also increase and V_{11}^+ cannot scale at the wall.

Conclusions

To conclude, we have simulated a Poiseuille turbulent channel flow at a friction Reynolds number of $Re_\tau = 10000$. This simulation was made in a small box of size $(2\pi h, 2h, \pi h)$, large enough to accurately compute the statistics of the flow. The profile of $\overline{U}$ shows a long log layer, extending from $y^+ \approx 400$ to $y^+ \approx 2500$. The value of the von Kármán constant is $\kappa = 0.394$. The first maximum of the streamwise profile u'^+ continues growing, which is the cause of the scaling failure of the dissipation at the wall. The second maximum of u'^+ has not appeared yet, and it is foreseen to appear at approximately $Re_\tau = 13500$. On the other hand, The turbulent budgets show a almost perfect scaling in the outer region with $B_{ij}^* = yB_{ij}/u_\tau^3$.

Acknowledgements

The authors gratefully acknowledge providing computing time on the Gauss Centre for Supercomputing e.V. on the GCS Supercomputer SuperMUC-NG at Leibniz Supercomputing Centre under project number pr92la, on the supercomputer Lichtenberg II at TU Darmstadt under project number project00072 and on the supercomputer CLAIX-2018 at RWTH-Aachen, project bund0008. MO would like to acknowledge her funding by the German Research Foundation (DFG) through the project OB96/39-1 and OB96/48-1. SH was supported by contract RTI2018-102256-B-I00 of MINECO/FEDER.

REFERENCES

Abe, H. & Antonia, R.A. 2016 Relationship between the energy dissipation function and the skin friction law in a turbulent channel flow. *Journal of Fluid Mechanics* **798**, 140–164.

Alcántara-Ávila, F., Hoyas, S. & Pérez-Quiles, M.J. 2021 Direct numerical simulation of thermal channel flow for $Re_\tau = 5000$ and $Prand = 0.71$. *Journal of Fluid Mechanics* **916**, A29.

Avsarkisov, V., Hoyas, S., Oberlack, M. & García-Galache, J.P. 2014*a* Turbulent plane Couette flow at moderately high reynolds number. *Journal of Fluid Mechanics* **751**, R1.

Avsarkisov, V., Oberlack, M. & Hoyas, S. 2014*b* New scaling laws for turbulent Poiseuille flow with wall transpiration. *Journal of Fluid Mechanics* **746**, 99–122.

Bernardini, M., Pirozzoli, S. & Orlandi, P. 2014 Velocity statistics in turbulent channel flow up to $Re_\tau = 4000$. *Journal of Fluid Mechanics* **758**, 327–343.

Hoyas, Sergio & Jiménez, Javier 2006 Scaling of the velocity fluctuations in turbulent channels up to $Re_\tau = 2003$. *Physics of Fluids* **18** (1), 011702.

Hoyas, S. & Jiménez, J. 2008 Reynolds number effects on the Reynolds-stress budgets in turbulent channels. *Physics of Fluids* **20** (10), 101511.

Hoyas, Sergio, Oberlack, Martin, Alcántara-Ávila, Francisco, Kraheberger, Stefanie V. & Laux, Jonathan 2022 Wall turbulence at high friction reynolds numbers. *Phys. Rev. Fluids* **7**, 014602.

Kim, J., Moin, P. & Moser, R. 1987 Turbulence statistics in fully developed channels flows at low Reynolds numbers. *Journal of Fluid Mechanics* **177**, 133–166.

Kraheberger, S., Hoyas, S. & Oberlack, M. 2018 Dns of a turbulent couette flow at constant wall transpiration up to $Re_\tau = 1000$. *Journal of Fluid Mechanics* **835**, 421–443.

Lee, M. & Moser, R. 2015 Direct numerical simulation of turbulent channel flow up to $Re_\tau \approx 5200$. *Journal of Fluid Mechanics* **774**, 395–415.

Lele, S. K. 1992 Compact finite difference schemes with spectral-like resolution. *Journal of Computational Physics* **103** (1), 16–42.

Lluesma-Rodríguez, F., Álcantara Ávila, F., Pérez-Quiles, M.J. & Hoyas, S. 2021 A code for simulating heat transfer in turbulent channel flow. *Mathematics* **9** (7).

Lozano-Durán, A. & Jiménez, J. 2014 Effect of the computational domain on direct simulations of turbulent channels up to $Re_\tau = 4200$. *Physics of Fluids* **26** (1), 011702.

Luchini, P. 2017 Universality of the turbulent velocity profile. *Physical Review Letters* **118** (22), cited By 26.

Mansour, N. N., Kim, J. & Moin, P. 1988 Reynolds-stress and dissipation-rate budgets in a turbulent channel flow. *Journal of Fluid Mechanics* **194**, 15.

Marusic, Ivan, Monty, Jason P., Hultmark, Marcus & Smits, Alexander J. 2013 On the logarithmic region in wall turbulence. *Journal of Fluid Mechanics* **716**, R3.

McKeon, B. J., Li, J., Jiang, W., Morrison, J. F. & Smits, A. J. 2004 Further observations on the mean velocity distribution in fully developed pipe flow. *Journal of Fluid Mechanics* **501**, 135–147.

Monkewitz, P.A. 2021 The late start of the mean velocity overlap log law at-a generic feature of turbulent wall layers in ducts. *Journal of Fluid Mechanics* **910**.

Oberlack, Martin, Hoyas, Sergio, Kraheberger, Stefanie V., Alcántara-Ávila, Francisco & Laux, Jonathan 2022 Turbulence statistics of arbitrary moments of wall-bounded shear flows: A symmetry approach. *Phys. Rev. Lett.* **128**, 024502.

Pope, S. B. 2000 *Turbulent flows*. Cambridge University Press.

Samie, M., Marusic, I., Hutchins, N., Fu, M.K., Fan, Y., Hultmark, M. & Smits, A.J. 2018 Fully resolved measurements of turbulent boundary layer flows up to $Re_\tau = 20000$. *Journal of Fluid Mechanics* **851**, 391–415.

Spalart, P.R. & Abe, H. 2021 Empirical scaling laws for wall-bounded turbulence deduced from direct numerical simulations. *Physical Review Fluids* **6** (4), cited By 0.

Spalart, Philippe R, Moser, Robert D & Rogers, Michael M 1991 Spectral methods for the Navier-Stokes equations with one infinite and two periodic directions. *Journal of Computational Physics* **96** (2), 297–324.

Yamamoto, Yoshinobu & Tsuji, Yoshiyuki 2018 Numerical evidence of logarithmic regions in channel flow at Re_τ = 8000. *Physical Review Fluids* **3**, 012602(R).